# Characterizing the Dimerizations of Phenalenyl Radicals by ab Initio Calculations and Spectroscopy: $\sigma$-Bond Formation versus Resonance $\pi$-Stabilization

**David Small,[†] Sergiy V. Rosokha,[‡] Jay K. Kochi,*[,‡] and Martin Head-Gordon*[,†]**

*Department of Chemistry, University of California, and Chemical Sciences Division, Lawrence Berkeley National Laboratory, Berkeley, California 94720, and Department of Chemistry, University of Houston, Houston, Texas 77204*

*Received: August 1, 2005; In Final Form: October 11, 2005*

Electronic-structure calculations for the self-association of phenalenyl radical (**P**$^{\bullet}$) predict the formation of dimeric species ($\sigma$-$\mathbf{P}_2$) in which both moieties are connected by a $\sigma$-bond with $r_{\mathbf{P-P}} \sim 1.59$ Å and bond dissociation enthalpy of $\Delta H_D \sim 16$ kcal mol$^{-1}$. Such an unusually weak $\sigma$-bond is related to the loss of aromatic stabilization energy of ~34 kcal mol$^{-1}$ per phenalenyl moiety, largely owing to rehybridization. Ab initio calculations also reveal that the corresponding (one-electron) bond between phenalenyl radical and its closed-shell cation in $\sigma$-$\mathbf{P}_2^{+\bullet}$ is unstable relative to dissociation. Time-dependent DFT computations indicate the absence of any (strongly allowed) electronic transition in the visible region of the absorption spectrum of phenalenyl $\sigma$-dimer. Such theoretical predictions are supported by experimental (ESR and UV−NIR) spectroscopic studies, in which the availability of a series of sterically hindered phenalenyl radicals allows definitive separations of the $\sigma$-dimerization process from interference by $\pi$-dimerization. As such, the thermodynamic parameters (determined from the temperature dependence of the ESR signals) with $\Delta H_D = 14$ kcal mol$^{-1}$ and $\Delta S_D = 52$ e.u. can be assigned to the formation of the colorless $\sigma$-dimer. Similar results are obtained for all phenalenyl derivatives (provided their substitution patterns allow $\sigma$-bond formation) to confirm the energetic preference of $\sigma$-dimerization over $\pi$-dimerization.

## 1. Introduction

Spontaneous self-associations of hydrocarbon radicals lead to isomeric pairs of dimers that are basically distinguished by their unique $\pi$- and $\sigma$-symmetric structures—the delineation of which is relevant to such diverse research areas as synthetic and mechanistic chemistry in solution as well as the preparation of new solid-state materials.[1,2] Detailed analyses of the two different modes of intermolecular (homolytic) interactions are also needed for understanding ordered/disordered transformations pertinent to magnetic and conductive properties of such organic materials as well as hydrocarbon growth in sooting flames[3] and the formation of carbonaceous grains in interstellar space.[4]

Accordingly, we now address the self-association issue using both computations and experiments in order to obtain insight into the fundamentals of $\pi$- and $\sigma$-dimerizations. For this study, our choice of the tricyclic phenalenyl radical is based on three reasons. First, it has special thermodynamic stability arising from the nonbonding character of its half-occupied orbital[5] so that both the neutral radical and the closed shell cation and anion are synthetically accessible.[6,7] Second, earlier experimental studies[8,9] indicate that the phenalenyl radical and its derivatives show both $\pi$- and $\sigma$-self-associations (Scheme 1). Third, these dimerizations play a key role in determining the condensation products of phenalenyl radicals[10] as well as the conducting, magnetic, and optical properties of the phenalenyl-based organic solids.[11,12]

**SCHEME 1**

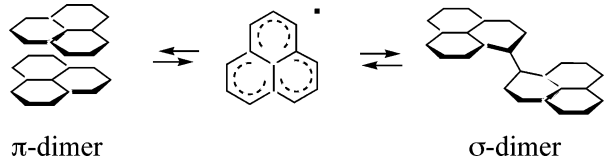


**CHART 1**

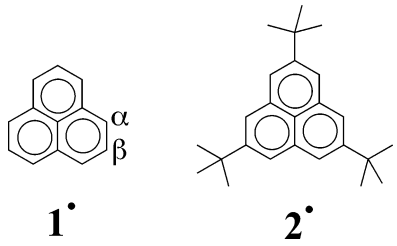


**1**$^{\bullet}$ **2**$^{\bullet}$

The possibility of both $\pi$- and $\sigma$-dimerization of phenalenyl radical requires special attention to the separation and unambiguous characterization of each process. Thus, the experimental characterization of $\pi$-dimerization is made possible by bulky *tert*-butyl substituents at the 2,5,8 positions to inhibit formation of the $\sigma$-dimer.[13,14] Indeed, X-ray studies of the substituted phenalenyl **2**$^{\bullet}$ (Chart 1) indicate that its $\pi$-dimer with a face-to-face stacking distance of only 3.2 Å is too short for a conventional van der Waals complex (>3.5 Å) but too long for any conventional covalent bond.[13] Solution studies reveal that such a $\pi$-dimerization is accompanied by enthalpy release of about 10 kcal mol$^{-1}$ (in dichloromethane) and the appearance of an intense electronic transition at $\lambda_{max} \sim 600$ nm.[14] Electronic structure calculations closely reproduce the experimental (struc-

* Corresponding authors. E-mail: mhg@cchem.berkeley.edu (M.H.-G.); jkochi@uh.edu (J.K.K.).
[†] University of California and Lawrence Berkeley National Laboratory.
[‡] University of Houston.

10.1021/jp054244n CCC: $30.25 
Published on Web 11/17/2005

tural, spectral and thermodynamic) results and identify the origin of this relatively long-bonded interaction as a dispersion-assisted (diradicaloid) two-electron bond that is highly delocalized over 12 centers.[14] As such, this $\pi$-stacking (enhanced by weak covalent interactions) constitutes an interesting new class of intermolecular interactions.[15] On the other hand, the temperature-dependent equilibrium between phenalenyl radical **1**• (Chart 1) and its diamagnetic counterpart, as measured by ESR spectroscopy, is related to $\sigma$-dimerization that ultimately leads to the formation of 1,1′-biphenalenyl and peropyrenes.[8,10,16] Recently, the $\sigma$-bonding between (copper- or boron-coordinated) phenalenyl moieties has been characterized by X-ray crystallography.[16,17] However, the pure $\sigma$-dimer of phenalenyl radical has not yet been isolated nor unambiguously identified; the spectral and thermodynamic characterization of $\sigma$-dimerization in solution remains uncertain owing to possible interference by the competing formation of $\pi$-dimer.

Our interests here are focused on calculations and experiments that characterize the nature of $\sigma$-dimers ($\sigma$-$\mathbf{P}_2$) derived from a pair of phenalenyl radicals. At first glance, the identification of $\sigma$-$\mathbf{P}_2$ seems to be relatively straightforward; from the point of view of first-principles calculations, this $\sigma$-dimer (which has not yet been addressed via ab initio calculations) should not have diradicaloid character previously found[14] in its $\pi$-bonded counterpart ($\pi$-$\mathbf{P}_2$). However, we will show that the dimeric $\sigma$-$\mathbf{P}_2$ is more complicated, and thus more interesting, than an ordinary $\sigma$-bonded molecule. This stems from the unusual stability of phenalenyl radical (**P**•) itself, due to its aromaticity, together with the nonbonding nature of the highest occupied radical orbital. If phenalenyl forms a $\sigma$-bond with another molecule, the extensive conjugation is partially destroyed, and this loss of delocalization energy will compete with $\sigma$-bond formation. In addition, the $\sigma$-dimer is more flexible than the $\pi$-dimer, and its structure will be determined by the $\sigma$-bond formed between chiral carbons. To complement these computational results, we also report experimental studies directed to the reversible formation of $\sigma$-dimers in which steric constraints resulting from the different placement of bulky substituents allow the clear separation and comparison of $\sigma$- and $\pi$-dimerizations.[18]

## 2. Computational Results

**2.1. Theoretical Methods.** The range of theoretical (ab initio) methods applicable to phenalenyl dimerization is limited by the significant size of the dimeric associates. In the previous study of phenalenyl $\pi$-dimers,[14] we employed the perfect-pairing method[19] with one electron pair (corrected by perturbation theory),[20] as the use of just one pair was the minimal appropriate treatment[21] owing to the small HOMO−LUMO gap of the $\pi$-dimer. However, the relatively large gap expected for the $\sigma$-dimer does not warrant any reduced level of perfect pairing. Therefore, we used basic self-consistent field (SCF) methods such as restricted Hartree−Fock (RHF) corrected with Moller−Plesset second order perturbation theory[22] (RMP2), unrestricted Hartree−Fock (UHF) along with UMP2, and Density Functional Theory (DFT) using the B3LYP functional[23] with unrestricted orbitals (UB3LYP). In all that follows, we use the term RHF in the usual context of closed-shell molecules and also to indicate a restricted-orbital Hartree−Fock calculation on a molecule with an unpaired electron.

**2. 2. Structure Optimization.** Simple Lewis-structure arguments exclude a stable $\sigma$-dimer that is bonded through two $\beta$ carbons or through one α and one $\beta$ carbon (see Chart 1). Each of the two principal $\sigma$-bonded α carbons is chiral and may be labeled R or S, so there are six distinct α/α-bonded structures.

**CHART 2**[a]

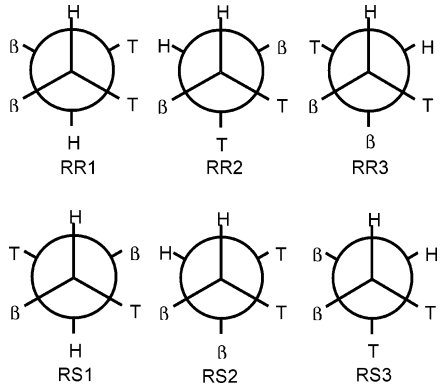


[a] "T" indicates a tertiary carbon (i.e., bonded to three other carbons).

**CHART 3**

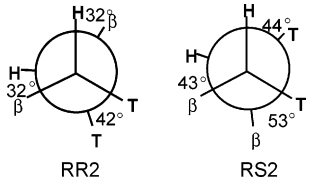


**TABLE 1: Binding Energies[a] for Isomers of the Phenalenyl $\sigma$-Dimer**

| method | RR1 | RR2 | RR3 | RS1 | RS2 |
|---|---|---|---|---|---|
| RHF[b] | 15.5 | 15.9 | 20.1 | 15.7 | 18.6 |
| RMP2[b] | 14.5 | 13.1 | 15.3 | 13.5 | 15.3 |
| UHF | −31.0 | −31.2 | −26.8 | −31.0 | −28.2 |
| UMP2 | 6.0 | 5.2 | 8.1 | 5.5 | 7.8 |
| UB3LYP | −1.1 | −1.1 | 2.1 | −1.1 | 0.9 |

[a] Calculated with 6-31G* basis (in kcal/mol). [b] ROHF was used to calculate the energy of **1**• (Chart 1).

The Newman projections taken through the principal $\sigma$-bond are shown in Chart 2. The energetic equivalence of the RS2 and RS3 projections limited the study to five distinct isomeric $\sigma$-dimers. Five starting structures were obtained with semiempirical methods in HyperChem.[24] All subsequently discussed calculations were performed with the Q-Chem program.[25] The geometries were then optimized at the RHF/6-31G* level. The resulting geometries of the five unique isomers (three RR and two RS) are included as PDB files in the Supporting Information. Interestingly, the optimized RR2 and RS2 structures have the somewhat distorted Newman projections shown in Chart 3.

Further optimizations of all five structures were completed at the UHF/6-31G* and UB3LYP/6-31G* levels, and the resulting binding energies (defined as the electronic energy change for dissociation) of the dimers are presented in Table 1 (including MP2/6-31G* results calculated at HF geometries).

**2.3. Refinement of the Binding Energies.** The wide discrepancy among the energies listed in Table 1 clearly indicates the necessity of their further refinement for adequate characterization of phenalenyl $\sigma$-dimerization. To obtain more conclusive values of the binding energies, we therefore decided to treat (Scheme 2) the phenalenyl dimerization as the sum of two transformations:

Such a splitting of the dissociation process (3) into subreactions 1 and 2 provided two advantages. First, the calculations involving the large phenalenyl dimer were confined to rather economical (HF, DFT, and perturbation theory) methods, which

**SCHEME 2**

$$\mathbf{P}_2 + C_2H_6 \rightarrow 2\,\mathbf{P}\text{-}CH_3 \quad (1)$$

$$2\,\mathbf{P}\text{-}CH_3 \rightarrow 2\,\mathbf{P}^{\bullet} + C_2H_6 \quad (2)$$

$$\mathbf{P}_2 \rightarrow 2\,\mathbf{P}^{\bullet} \quad (3)$$

typically excel in dealing with isogyric and isodesmic[26] processes such as (1), in contrast to (3). Second, the nonisodesmic (bond-breaking) and non-isogyric (2), which required more accurate methods, now involves much smaller molecules than (3). As such, it was treated with Coupled-Cluster Singles Doubles with Perturbative Triples,[27] or CCSD(T) methodology, which consistently provides highly accurate results for a variety of applications.[28] Furthermore, for computational practicality, we froze the core electrons in all molecules in (2) and used a mixed basis set: (i) 6-31G* orbitals for the two main $\sigma$-bonded carbon atoms in **P**-$CH_3$ and in $C_2H_6$ and (ii) 6-31G orbitals for the remaining atoms. In this way, the electronic energy change for (2) was calculated as 17.4 kcal mol$^{-1}$. Accordingly, the addition of this value to the electronic energy change in (1) shown in column 2 of Table 2 (as calculated by the different methods indicated in column 1) led to the overall $\sigma$ binding energy, which is displayed for the RR3 isomer in Table 2 (the corresponding data for the other structures are presented in the Supporting Information). The binding energies of different isomers (all calculated using the RMP2 results for reaction 1) are shown in Table 3.

For comparison with the experimental enthalpies (vide infra), we took into account the zero-point vibrational energies of the $\sigma$-dimer and the monomer as well as an estimate of residual basis set error. With the RR3-isomer of $\sigma$-$\mathbf{P}_2$ taken as an example, a frequency calculation with B3LYP/6-31G* showed that the dimer zero point was 3.4 kcal mol$^{-1}$ above the doubled value of monomer. It thus led to the enthalpy change for $\sigma$-dimerization of 18.2 kcal mol$^{-1}$, as compared with the uncorrected value of 21.6 kcal mol$^{-1}$ in Table 2. We evaluated the basis set error with two steps: (a) we calculated the electronic energy change of transformation (3) with the significantly larger cc-pVTZ basis set. The best method that is practical for this is MP2, which we used in the RMP2 form with the resolution of the identity approximation;[29] (b) with RMP2, we calculated the electronic energy change of transformation (3) with the smaller basis sets used above. This was done by using 6-31G* to calculate the electronic energy change for transformation (1) and using the same mixed basis-set used in the CCSD(T) calculations to obtain the electronic energy change for (2) and then adding the results. The difference between the energies from step (a) and step (b) gives an estimate of the basis set extension effect. Step (a) gave a binding energy of 14.0 kcal mol$^{-1}$ while step (b) gave 16.3 kcal mol$^{-1}$, leading to a basis set error of 2.3 kcal mol$^{-1}$. As such, a final approximation for the enthalpy change for the dissociation of $\sigma$-$\mathbf{P}_2$ with good basis set was taken as $\Delta H = 18.2 - 2.3 = 15.9$ kcal mol$^{-1}$. The corrected binding enthalpies of the five isomers are given in Table 3. We also mention that the step (b) result of 16.3 kcal mol$^{-1}$ is consistent with the result obtained using 6-31G*, which is 15.3 kcal mol$^{-1}$ (see Table 1). We believe this justifies the use of our slightly expanded 6-31G basis for transformation (2). Interestingly, while earlier computations[14] predicted the energetically favorable (face-to-face) associate of phenalenyl radical with its closed-shell cation to form the paramagnetic $\pi$-dimer ($\pi$-$\mathbf{P}_2^{+\bullet}$), all our attempts failed to find the stable paramagnetic $\sigma$-bonded dimeric species ($\sigma$-$\mathbf{P}_2^{+\bullet}$). Several metastable cationic $\sigma$-dimer structures were obtained starting from the various enantiomeric geometries described above, but in all cases their energies were several kcal mol$^{-1}$ higher than that of separate (dissociated) species.

**TABLE 2: Electronic Energy Change (kcal mol$^{-1}$) for Transformation (1) and Binding Energy for the RR3 Dimer**

| method | $\Delta E(1)^a$ | $E(\mathrm{RR3})^b$ |
|---|---|---|
| RHF | −1.88 | 15.47 |
| RMP2 | 4.25 | 21.60 |
| UHF | −1.58 | 15.77 |
| UMP2 | 2.87 | 20.22 |
| UB3LYP | −1.19 | 16.16 |

[a] For (1) in Scheme 2 computed by the method in column 1 and 6-31G* basis. [b] Obtained by adding electronic energy for (2) in Scheme 2 to the result in column 1.

**TABLE 3: Binding Energies[a] and Corrected Enthalpies (kcal mol$^{-1}$) of Various $\sigma$-Dimers**

| isomer | energy | enthalpy |
|---|---|---|
| RR1 | 20.83 | 14.75 |
| RR2 | 19.37 | 14.18 |
| RR3 | 21.60 | 15.90 |
| RS1 | 19.82 | 12.61 |
| RS2 | 21.61 | 16.42 |

[a] Based on RMP2 results for (1) in Scheme 2.

**2.4. Spectral Calculations.** To analyze the spectra of the $\sigma$-dimers, we followed our earlier computational approach based on time-dependent density functional theory[30] (TDDFT) using UB3LYP/6-31G*. This method predicted the lowest energy transition for all the isomers at about 2.4 eV with negligible (0.0) oscillator strengths. The strongest excitations were found to be between 3.5 and 4.0 eV, and the corresponding energies and oscillator strengths are given in Table 4.

## 3. Experimental Results

Steric control of $\pi$- and $\sigma$-dimerization was readily modulated by the judicious placement of a pair of bulky *tert*-butyl substitutents in the phenalenyl radicals **3** and **4** illustrated in Chart 4;[31] and the temperature dependence of their spectroscopic behavior in dichloromethane solutions was compared with those of phenalenyl radicals **1** and **2** (Chart 1) in the following manner.

**3.1. ESR Spectroscopy of Phenalenyl Dimerization.** ESR spectra of the phenalenyl radicals in Chart 1 were characterized (in dichloromethane, chloroform, or toluene solutions) by well-resolved (proton) hyperfine splittings. For example, radical **1**$^{\bullet}$ showed a binomial septet, with each line further split into

**TABLE 4: TDDFT-Calculated Energies ($h\nu$) and Oscillator Strengths (OS) of Strongest Electronic Transition in Different Isomers of the $\sigma$-Bonded Phenalenyl Dimer[a]**

| isomer | $h\nu$ (eV) | OS |
|---|---|---|
| RR1 | 3.6 | 0.23 |
| RR2 | 4.0 | 0.17 |
| RR3 | 3.6 | 0.25 |
| RS1 | 3.5 | 0.30 |
| RS2 | 3.5 | 0.14 |

[a] All results computed at RHF/6-31G* optimized geometries.

**CHART 4**

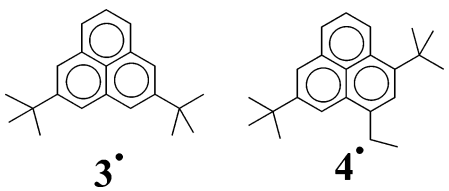

**3**$^{\bullet}$ **4**$^{\bullet}$

**TABLE 5: ESR Spectra of Various Phenalenyl Radicals**

| radical | $a_H(G)^a$ | |
|---|---|---|
| **1**• [b] | 6.3(6) | 1.8(3) |
| **2**• [c] | 6.2(6) | |
| **3**• | 6.2(6) | 1.8(1) |
| **4**• | 6.1(4) | 1.9(2) |

[a] In parentheses: number of equivalent protons. [b] From Gerson in ref 8b. [c] From Goto et al. in ref 13a.

quartets in the ratio of 1:3:3:1, in accord with the splitting by two sets of equivalent ($\alpha$ and $\beta$) protons.[8b] By contrast, due to substitution of every apical hydrogen, the ESR spectrum of **2**• showed only a well-resolved binomial septet related to 6 equivalent $\alpha$-protons.[13,14] Analogously, the ESR spectra of radicals **3**•and **4**• (Chart 4) agree with their structural details, and the hyperfine splitting constants (derived from computer simulation) are presented in Table 5.

While the hyperfine splittings and line widths of the ESR spectra of all radicals remained singularly invariant with temperature variations, their signal intensities dropped significantly upon cooling (Figures S1 and S2 in Supporting Information) in contrast to that expected from of the Curie−Weiss behavior. Temperature-dependent intensity changes were quite reversible, and deviations from Curie−Weiss behavior became more pronounced with increasing initial concentrations of the radical. As such, ESR-intensity variations were assigned to the reversible formation of diamagnetic (ESR-silent) dimers,[8,14,16] e.g.

$$\mathbf{4}^{\bullet} + \mathbf{4}^{\bullet} \rightleftarrows \mathbf{4}_2 \qquad (4)$$

Indeed, the double integration of the ESR spectra allowed us to quantitatively evaluate the fraction ($\alpha_M$) of the phenalenyl monomer according to eq 4, and this procedure led to the dimerization constants whose linear dependences with inverse temperature (Figure 1) afforded the thermodynamic parameters listed in Table 6.

Thus ESR measurements showed that the formation of the diamagnetic dimer was a characteristic for all phenalenyl radicals, but it did not reveal the dimerization mode. The pattern of *tert*-butyl (steric) hindrances was helpful in this respect, since only $\pi$-dimer formation is viable for radical **2**• and only $\sigma$-dimer formation for **4**•. By contrast, both pathways were possible for derivatives **1**• and **3**•. Electronic spectroscopy allowed us to resolve this ambiguity in the following manner.

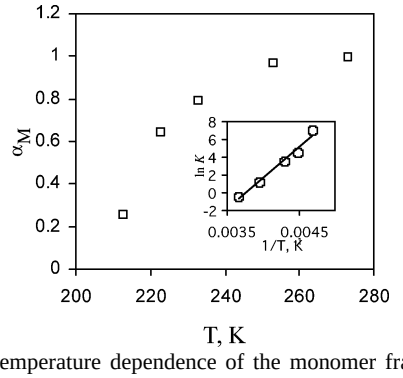


**Figure 1.** Temperature dependence of the monomer fraction $\alpha_M$ in dichloromethane solution of radical **4**• ($c_0 = 2$ mM)l$_2$. Inset: temperature dependence of the dimerization constant *K*.

**TABLE 6: Thermodynamics of Phenalenyl Dimer Dissociation[a]**

| radical | $\Delta H_D$ (kcal mol$^{-1}$)[b] | $\Delta S_D$ (e.u.)[c] |
|---|---|---|
| **1**• | 10 | 18 |
| **2**• [d] | 9.5 | 36 |
| **4**• [e] | 14 | 52 |

[a] In $CH_2Cl_2$ unless otherwise noted. [b] Error ≅ 1 kcal/mol. [c] Error ≅ 4 e.u. (1 e.u. = 4.184 J K$^{-1}$ mol$^{-1}$). [d] From ref 14. [e] In $CDCl_3$.

**3.2. Electronic Spectroscopy of Phenalenyl Dimerization.** The tri-*tert*-butyl-substituted radical **2**• was characterized by a visible absorption at $\lambda_{max} = 540$ nm with $\epsilon = 10^2$ M$^{-1}$ cm$^{-1}$.[13a] In addition to this rather weak band, solutions of radical **2**• revealed another absorption band at $\lambda_{max} \sim 595$ nm, which showed quadratic concentration dependence and grew dramatically upon lowering the temperature [In this way, the slightly pink solution took on an intense blue color].[14] Quantitative analysis of electronic-spectroscopy data, together with the foregoing ESR results and solid-state absorption measurements allowed the assignment of this additional intense absorption band ($\epsilon = 2 \times 10^4$ M$^{-1}$ cm$^{-1}$) to the diamagnetic $\pi$-dimer (**$\pi$-2**$_2$).[14]

By way of comparison, the substituted phenalenyl radical **4**• was practically colorless in dichloromethane solutions and showed only a weak band at $\lambda_{max} \sim 550$ nm ($\epsilon \sim 10^2$ M$^{-1}$ cm$^{-1}$). Importantly, these solutions remained colorless upon lowering the temperature to −90 °C, and the electronic spectrum confirmed that no new absorption band appeared in the visible range. Such an observation was consistent with the fact that a pair of *tert*-butyl and one ethyl substituent in **4**• prevented the staggered arrangement, which was required for the formation of the intensely colored $\pi$-dimer. Nevertheless, ESR measurements showed that lowering the temperature of such a solution was accompanied by the shift of the equilibrium from monomer **4**• to the diamagnetic dimer (as evidenced by an practically ESR-silent spectra at −90 °C). We therefore concluded that because the dimerization of radical **4**• proceeded without the appearance of any intense band in visible range, it must have involved the formation of a $\sigma$-bond, corresponding to the colorless species **$\sigma$-4**$_2$.

In the same manner, the electronic spectroscopy of the **1**• and **3**• revealed that no new absorption (visible−NIR) band appeared when the temperature was lowered from +20 °C to −90 °C.[32] Such an observation, together with ESR data that showed shifts from paramagnetic to diamagnetic species upon the temperature decrease, indicated that the self-association of these radicals also resulted in the formation of the colorless $\sigma$-bonded (diamagnetic) dimer.

**3.3. Intermolecular Interaction of Phenalenyl Radical with Its Closed-Shell Cation.** To further study the different modes of phenalenyl-radical dimerization, we turned to their intermolecular interaction with its closed-shell cationic counterpart. As reported earlier,[9] the addition of phenalenyl cation (**1**$^+$) to the solution of phenalenyl radical (**1**•) results in the appearance of the doubled ESR spectrum, and the electronic spectrum shows a new NIR band around 1900 nm that is absent in the separately measured spectra of the phenalenyl radical and cation. Such spectral effects are analogous to those accompanying the formation of the paramagnetic $\pi$-dimer (**$\pi$-2**$_2^{+\bullet}$) from the mixture of radical **2**• and cation **2**$^+$ [14] and leads to a conclusion that the dimeric **$\pi$-1**$_2^{+\bullet}$ is formed according to

$$\mathbf{1}^{\bullet} + \mathbf{1}^{+} \rightleftarrows \pi\text{-}\mathbf{1}_2^{\bullet +} \qquad (5)$$

By contrast, the solution containing both radical **4**• and the corresponding cation **4**$^+$ (in which the $\pi$-interaction is prohibited by steric factors) does not show any new band in the 1000−3000 nm range, and the ESR spectrum reveals only a broad unresolved signal. [It should be noted, that the **1**•/**1**$^+$, **3**•/**3**$^+$, and **4**•/**4**$^+$ systems are quite unstable and prevent the quantitative analysis of the thermodynamics of intermolecular interactions.] Overall, these data on the interaction of phenalenyl radical and

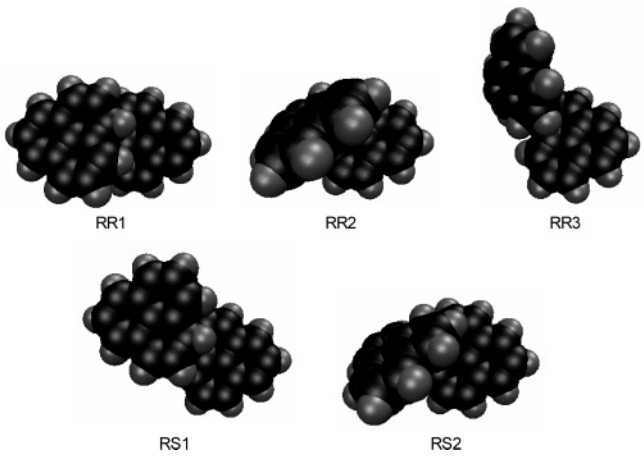


**Figure 2.** Calculated structures of the $\sigma$-bonded phenalenyl dimer.

its cation indicate that the (one-electron-bonded) paramagnetic $\pi$-dimeric species is formed, when a (face-to-face) approach is feasible.

## 4. Discussion

It is now possible to use the ab initio quantum mechanical evaluations of phenalenyl $\sigma$-dimerization to support and extend the experimental results with respect to (1) structure, (2) energetics, (3) electronic transitions, and (4) competition between $\pi$ and $\sigma$ dimerization, as follows.

**4.1. Structure of Phenalenyl $\sigma$-Dimer.** There are five distinct isomers of the phenalenyl $\sigma$-dimer as shown in Figure 2. These are energetically distinguished essentially by two factors: steric repulsion and intermolecular dispersion. The distinctions between these isomers may be rationalized by examining their geometries as shown in PDB files in the Supporting Information. The primary $\sigma$-bond lengths for RR3, RS2, RR2, RS1, and RR1 are 1.575, 1.579, 1.585, 1.593, and 1.596 Å, respectively. This is exactly the ordering one would expect from the RHF binding energies of these isomers in row 1 of Table 1 (i.e., the higher the binding energy, the smaller the bond length). Since RHF does not model dispersion, this is solely the effect of steric repulsion, of which RR3 has the least. As we take these same geometries and perform higher order computations (e.g., MP2), the steric repulsions do not change but the binding energy ordering is altered due to the inclusion of effects of dispersion (i.e., the weak attractive van der Waals attractions between atoms in the two different phenalenyl ring systems that are not in steric contact). From Figure 2, the order of dispersion from highest to lowest amount should go roughly as RR1 > RS1 > RS2 $\approx$ RR2 > RR3. This is completely consistent with the data in row 2 of Table 1 (i.e., it explains why RR1 becomes favored over RS1 and RR2, why RS1 becomes favored over RR2, and why RS2 becomes as stable as RR3 as we move from row 1 to row 2).

We note that the primary $\sigma$-bond lengths are similar to the corresponding bond lengths established in X-ray structural studies of $\sigma$-bonded phenalenyl moieties in spirobiphenalenyls (1.599 Å)[17] and in copper complexes of azaphenalenyls (1.583 Å).[16] Although such bond lengths are slightly longer than standard $C(sp^3)-C(sp^3)$ bonds (1.54 Å), the Cambridge Crystallographic Database contains numerous examples of such elongations in various types of stable organic molecules.

**4.2. Energetics of Phenalenyl $\sigma$-Dimerization.** The phenalenyl $\sigma$-dimer is computed to have a bond dissociation enthalpy of $\sim$16 kcal mol$^{-1}$. Interestingly, the latter is not much larger than that (10 kcal mol$^{-1}$) previously computed for the weak $\pi$-bonding of the same pair of phenalenyl radicals at the relatively wide (equilibrium) separation of 3.2 Å. The direct computation of this energy change is difficult, and low-level standard (RHF, UHF, UB3LYP, RMP2, and UMP2) methods result in widely varying energetics (Table 1). On the other hand, the splitting into two processes (1) and (2) as presented in Scheme 2 allows us to overcome the computational difficulties of phenalenyl dimerization, since the above-mentioned methodologies perform substantially better for the isogyric and isodesmic (1), whereas the bond-breaking in (2) can be treated with the more accurate CCSD(T) method. Thus, RHF, UHF, and UB3LYP give remarkably consistent energies for (1), while RMP2 and UMP2 show mild relative shifts in favor of the reactants of (1). A distinctive attribute of MP2 is its ability to represent dispersion interactions, in contrast to DFT.[33] Because these interactions are dependent on molecular size, we believe that this explains the preference of the MP2 results for the reactants owing to the $\sigma$-dimer, which is clearly larger than the product of (1).

Most important, however, is the fact that such splittings in Scheme 2 allows us to consistently estimate the enthalpy of the primary $\sigma$-bond in the phenalenyl dimer as $\sim$ 16 kcal mol$^{-1}$ (after appropriate zero-point and basis set error corrections), which is well below that of a typical carbon−carbon bond of about 83 kcal mol$^{-1}$. Upon inspection of the $\sigma$-dimer structure, it is apparent that the energetically favored formation of the $\sigma$-bond upon dimerization is accompanied by the loss of aromaticity in phenalenyl monomers. The energy penalty of this loss can be approximated by comparison with the following:

$$\mathbf{P}-CH_3 \rightarrow \mathbf{P}^{\bullet} + CH_3^{\bullet} \qquad (6)$$

The enthalpy change for (6) as computed using CCSD(T) with the mixed 6-31G/6-31G* basis described above (with incorporated zero-point energies and basis set error correction) is 48.6 kcal mol$^{-1}$. Since the breaking of a C−C bond requires about 83 kcal mol$^{-1}$, the enthalpy related to the loss of aromaticity is approximately 34 kcal mol$^{-1}$. Because both monomers lose aromaticity in the process of $\sigma$-dimer formation, the enthalpy change by dissociation is $83-2 \times 34 = 15$ kcal mol$^{-1}$, which is consistent with the value of $\sim$16 kcal mol$^{-1}$ computed in section 2.3.

**4.3. Electronic Transitions in Phenalenyl $\sigma$-Dimers.** Time-dependent DFT results in section 2.4 indicate that the phenalenyl $\sigma$-dimer is characterized by negligible absorption in the visible region of the spectrum—in accord with the experimental results. Indeed, calculations show that significant excitation of phenalenyl $\sigma$-dimer occurs only at UV energies beyond 3.5 eV, which is in striking contrast to the strongly allowed NIR absorption of the phenalenyl $\pi$-dimer established earlier (both computationally and experimentally).

**4.4 $\sigma$- versus $\pi$-Dimerization.** The computational and experimental results of this study thus complement the earlier data[14] and allow quantitative comparison of the different modes of $\pi$- and $\sigma$-self-association. Spectral studies establish that intermolecular interaction of two phenalenyl radicals leads to $\sigma$-dimer provided this mode is not barred by steric hindrance. Such a clear preference of $\sigma$- over $\pi$-dimerization is partially due to an enthalpy factor—the $\sigma$-bond formation being somewhat higher than that of $\pi$-dimerization as estimated both by computation (16 and 10 kcal$^{-1}$mol$^{-1}$ for $\sigma$- and $\pi$-dimers, respectively) and spectroscopic measurements (9 kcal mol$^{-1}$ for $\pi$-dimer and 10−14 kcal mol$^{-1}$ for $\sigma$-dimer of different substituted phenalenyls). [Note that the enthalpy of $\pi$-dimer formation is associated with a "bond length" that is twice that

in the $\sigma$-dimer.] In addition, the relatively high and negative entropy change of −33 e.u for $\pi$-dimer formation[14] (which is related to the very specific staggered face-to-face approach required for such process) favors the conformationally flexible $\sigma$-dimer.

Finally, spectral studies show that in contrast to the diamagnetic dimer derived from radical/radical coupling, the related process of radical interaction with its closed-shell cation leads to formation of paramagnetic $\pi$-dimeric species (if sterically allowed) with characteristic doubled ESR spectra and an associated NIR absorption band. This observation is consistent with our computations showing that the (one-electron bonded) $\sigma$-dimer formed by phenalenyl radical and cation is unstable relative to dissociation. Indeed, for the $\pi$-dimeric species, the removal of one bonding electron (which is equivalent to the replacement of a radical by a cation and therefore loss of some covalent character) is well-compensated by the stabilizing electrostatic interaction in $\pi$-$\mathbf{P}_2^{+\bullet}$ relative to $\pi$-$\mathbf{P}_2$.[14] By comparison, the absence of such an stabilization ensures that $\sigma$-$\mathbf{P}_2^{+\bullet}$ is merely a metastable species, at best.

In summary, the availability of sterically hindered phenalenyl radicals allows us to separate and characterize the formation of the strongly colored $\pi$-dimer ($\pi$-$\mathbf{2}_2$), as well as the colorless $\sigma$-dimer ($\sigma$-$\mathbf{4}_2$). Importantly, if both $\sigma$- and $\pi$-interactions are sterically allowed, as in $\mathbf{1}^{\bullet}$, the 2-electron interaction via the radical/radical interaction results in preferential formation of diamagnetic colorless $\sigma$-dimers (although the thermodynamic parameters of both types of dimerization are comparable). In contrast, for the 1-electron radical/cation interaction of $\mathbf{1}^{\bullet}/\mathbf{1}^{+}$, the paramagnetic associate is preferred. This experimental observation is consistent with electronic-structure calculations, which successfully predict the structural, thermodynamic and spectroscopic features of dimeric associates of phenalenyl radicals.

## 5. Calculation Details

All SCF calculations used a wave function error tolerance of $10^{-8}$. Geometry optimizations used a maximum gradient component tolerance of $3 \times 10^{-4}$ hartree/Å, a maximum atomic displacement tolerance of $1.2 \times 10^{-3}$ Å, and an energy change tolerance of $10^{-6}$ hartree. All DFT calculations used a Euler−Maclaurin−Lebedev quadrature grid with 150 radial points and 302 angular points per radial point. All resolution of the identity MP2 calculations used the Ahlrichs cc-pVTZ auxiliary basis.[29]

## 6. Experimental Section

Solvents were purified according to standard laboratory procedures[34] and stored in Schlenk flasks under an argon atmosphere. *p*-Chloranil was purified by repeated recrystallization and used for the preparation of the phenalenyl radicals **1**−**4** illustrated in Charts 1 and 3 from their parent donors.[31]

ESR measurements were performed under an argon atmosphere on either a Bruker ESR-300 X-band or Varian E-line Century 100 spectrometers from +20 to −90 °C in EPR tubes equipped with a Teflon valve. The intensity of the ESR signals ($I_{EPR}$) was determined by double integration of the averaged spectra after baseline correction. The fraction of monomer ($\alpha_M$) in solution of $\mathbf{P}^{\bullet}$ was determined from the value of $I_{EPR}$ that was normalized as described earlier[14] (to account the temperature variation related to Curie law and instrumental factors). Equilibrium constant $K_D$ was calculated as: $K_D = (1 - \alpha_M)/2c_R\alpha_M^2$, where $c_R$ is the overall concentration of $\mathbf{P}^{\bullet}$ added to solution; the thermodynamic parameters for dimerization were calculated by the least-squares procedure from the dependence of $\ln(K_D)$ with $1/T$.

Electronic spectroscopy was carried out on either a HP 8453 spectrophotometer or with a Cary 500 spectrometer using a Dewar equipped with quartz lens. The cell was equipped with a Teflon valve fitted with Viton O-rings as described earlier.[14]

**Acknowledgment.** We thank V. Zaitsev for the preparation of phenalenyl radicals **1**−**4**. S.V.R. and J.K.K. (Houston) thank the R. A. Welch Foundation and the National Science Foundation for financial support. D.S. and M. H.-G. (Berkeley) were supported by the Director, Office of Energy Research, Office of Basic Energy Sciences, Chemical Sciences Division of the U.S. Department of Energy under Contract DE-AC03-76SF00098, Grant NNGO4GB94G from NASA's Long Term Space Astrophysics Program, and supercomputer time from NERSC.

**Supporting Information Available:** Dimerization energetics (Tables S1−S4), $\langle S^2 \rangle$ values for the unrestricted calculations (Table S5), and geometries of the three unique RR- and two unique RS-isomers of $\sigma$-$\mathbf{P}_2$ (PDB files), and the temperature-dependent ESR spectra of radicals $\mathbf{4}^{\bullet}$ (Figure S1) and $\mathbf{1}^{\bullet}$ (Figure S2). This material is available free of charge via the Internet at http://pubs.acs.org.

## References and Notes

(1) (a) Ingold, K. U. In *Free Radicals*, Vol. 1; Kochi, J. K., Ed.; Wiley: New York, 1973; p 39 ff. (b) Benson, S. W. *Adv. Photochem.* **1964**, *2*, 1. (c) Trogler, W. C., Ed. *Organometallic Radical Processes*; Elsevier: New York, 1990.

(2) (a) Farges, J.-P., Ed. *Organic Conductors*: *Fundamentals and Applications*; Marcel Dekker: New York, 1994. (b) Lahti, P. M., Ed. *Magnetic Properties of Organic Materials*; Marcel Dekker: New York, 1999.

(3) Frenklach, M. *Phys. Chem. Chem. Phys.* **2002**, *4*, 2028−2037.

(4) (a) Salama, F.; Galazutdinov, G. A.; Krelowski, J.; Allamandola, L. J.; Musaev, F. A. *Astrophys. J.* **1999**, *526*, 265. (b) Snow, T. P. *Spectrochim. Acta A* **2001**, *57*, 615−626.

(5) Haddon, R. C. *Aust. J. Chem.* **1975**, *28*, 2343.

(6) (a) Reid, D. H. *Quarter. Rev.* **1965**, *19*, 274. (b) Murata, I. In *Topics in Nonenzenoid Aromatic Chemistry*; Nozoe, T., Breslow, R., Hafner, K., Ito, S., Murata, I., Eds.; Wiley: Tokyo, 1973; Vol. 1, pp 159−190.

(7) (a) Due to this aromatic stability, the closed-shell cations from large numbers of polycyclic aromatic hydrocarbons have been observed as prominent peaks in the in-situ mass spectra of sooting flames.[7b−e] Additionally, it has been speculated that they may well be present in the interstellar medium,[7d] and first-principles electronic structure calculations of their vibrational[7d] and electronic[7e] spectra have been reported. (b) Weilmunster, P.; Keller, A.; Homann, K. H. *Combust. Flame* **1999**, *116*, 62−83. (c) Ahrens, J.; Keller, A.; Kovacs, R.; Homann, K. H. *Phys. Chem. Chem. Phys.* **1998**, *102*, 1823−1839. (d) Fetzer, J. C.; Kershaw, J. R. *Fuel* **1995**, *74*, 1533−1536. (e) Wornat, M. J.; Ledesma, E. B.; Marsh, N. D. *Fuel* **2001**, *80*, 1711−1726. (f) Hudgins, D. M.; Bauschlicher, C. W.; Allamandola, L. J. *Spectroc. Acta Pt. A* **2001**, *57*, 907−930. (g) Weisman, J. L.; Lee, T. J.; Head-Gordon, M. *Spectrochim. Acta A* **2001**, *57*, 931−945.

(8) (a) Reid, D. H. *Tetrahedron* **1958**, *3*, 339−352. (b) Gerson, F. *Helv. Chim. Acta* **1966**, *5*, 1463−1467. (c) Reid, D. H. *Chem. Ind.* **1956**, 1504. (d) Sogo, P. B.; Nakazaki, M.; Calvin, M. *J. Chem. Phys.* **1957**, *26*, 1343.

(9) Paskovich, D. H.; Reddoch, A. H. *J. Am. Chem. Soc.* **1972**, *94*, 6938.

(10) Pogodin, S.; Agranat, I. *J. Am. Chem. Soc.* **2003**, *125*, 12829.

(11) (a) Chi, X.; Itkis, M. E.; Patrick, B. O.; Barklay, T. M.; Reed, R. W.; Oakley, R. T.; Cordes, A. W.; Haddon, R. C. *J. Am. Chem. Soc.* **1999**, *121*, 10395. (b) Chi, X.; Itkis, M. E.; Kirschbaum, K.; Pinkerton, A. A.; Oakley, R. T.; Cordes, A. W.; Haddon, R. C. *J. Am. Chem. Soc.* **2001**, *123*, 4041. (c) Koutentis, P. A.; Chen, Y.; Cao, Y.; Best, T. P.; Itkis, M. E.; Beer, L.; Oakley, R. T.; Cordes, A. W.; Brock, C. P.; Haddon, R. C. *J. Am. Chem. Soc.* **2001**, *123*, 3864. (d) Pal, S. K.; Itkis, M. E.; Reed, R. W.; Oakley, R. T.; Cordes, A. W.; Tham, F. S.; Siegrist, T.; Haddon, R. C. *J. Am. Chem. Soc.* **2004**, *126*, 1478.

(12) (a) Itkis, M. E.; Chi, X.; Cordes, A. W.; Haddon, R. C. *Science* **2002**, *296*, 1443. (b) Miller, J. S. *Angew. Chem. Int. Ed.* **2003**, *42*, 27. (c) Tomoviæ, Ž.; Müllen, K. *Angew. Chem., Int. Ed.* **2004**, *43*, 755.

(13) (a) Goto, K.;, Kubo, T.; Yamamoto, K.; Nakasuji, K.; Sato, K.; Shiomi, D.; Takui, T.; Kubota, M.; Kobayashi, T.; Yakusi, K.; Ouyang, J. *J. Am. Chem. Soc.* **1999**, *121*, 1619. (b) Fukui, K.; Sato, K.; Shiomi, D.;

Takui, T.; Itoh, K.; Gotoh, K.; Kubo, T.; Yamamoto, K.; Nakasuji, K.; Naito, A. *Synth. Met.* **1999**, *103*, 2257. (c) Morita, Y.; Aoki, T.; Fukui, K.; Nakazawa, S.; Tamaki, K.; Suzuki, S.; Fuyuhiro, A.; Yamamoto, K.; Sato, K.; Shiomi, D.; Naito, A.; Takui, T.; Nakasuji, K. *Angew. Chem., Int. Ed.* **2002**, *41*, 1793. (d) Takano, Y.; Taniguchi, T.; Isobe, H.; Kubo, T.; Morita, Y.; Yamamoto, K.; Nakasuji, K.; Takui, T.; Yamaguchi, K. *J. Am. Chem. Soc.* **2002**, *124*, 11122. (e) Takano, Y.; Taniguchi, T.; Isobe, H.; Kubo, T.; Morita, Y.; Yamamoto, K.; Nakasuji, K.; Takui, T.; Yamaguchi, K. *Chem. Phys. Lett.* **2002**, *358*, 17.

(14) Small, D.; Zaitsev, V.; Jung, Y.; Rosokha, S. V.; Head-Gordon, M.; Kochi, J. K. *J. Am. Chem. Soc.* **2004**, *126*, 13850−13858.

(15) Similar bonding occurs in other radical $\pi$-dimers, such as $(TCNE)_2^{2-}$. See: (a) Novoa, J. J.; Lafuente, P.; Del Sesto, R. E.; Miller, J. S. *Angew. Chem., Int. Ed.* **2001**, *40* 2540−2545. (b) Del Sesto, R. E.; Miller, J. S.; Lafuente, P.; Novoa, J. J. *Chem. Eur. J.* **2002**, *8*, 4894−4908. (c) Lu, J. M.; Rosokha, S. V.; Kochi, J. K. *J. Am. Chem. Soc.* **2003**, *125*, 12161−12171. (d) Jakowski, J.; Simons, J. *J. Am. Chem. Soc.* **2003**, *125*, 16089. (e) Jung, Y.; Head-Gordon, M. *Phys. Chem. Chem. Phys.* **2004**, *6*, 2008−2011.

(16) Zheng, S.; Lan, J.; Khan, S. I.; Rubin, Y. *J. Am. Chem. Soc.* **2003**, *125*, 5786.

(17) Liao, P.; Itkis, M. E.; Oakley, R. T.; Tham, F. S.; Haddon, R. C. *J. Am. Chem. Soc.* **2004**, *126*, 14297.

(18) Use of bulky *tert*-butyl groups to sterically inhibit $\sigma$-dimerization of aromatic radicals was first described by Griller, D.; Ingold, K. U. *Acc. Chem. Res.* **1976**, *9*, 13.

(19) Goddard, W. A.; Harding, L. B. *Annu. Rev. Phys. Chem.* **1978**, *49*, 363−396.

(20) Nakano, H. *J. Chem. Phys.* **1993**, *99*, 7983.

(21) (a) Schmidt, M. W.; Gordon, M. S. *Annu. Rev. Phys. Chem.* **1998**, *49*, 233−266. (b) Jung, Y. S.; Head-Gordon, M. *J. Phys. Chem. A* **2003**, *107*, 7475−7481.

(22) Knowles, P. J.; Andrews, J. S.; Amos, R. D.; Handy, N. C.; Pople, J. A. *Chem. Phys. Lett.* **1991**, *186*, 130−136.

(23) (a) Becke, A. D. *J. Chem. Phys.* **1993**, *98*, 5648−5652. (b) Hertwig, R. H.; Koch, W. *Chem. Phys. Lett.* **1997**, *268*, 345−351.

(24) *HyperChem Professional 5.1*; Hypercube, Inc.: 1115 NW 4th Street, Gainesville, FL 32601.

(25) Kong, J.; White, C. A.; Krylov, A. I.; Sherrill, D.; Adamson, R. D.; Furlani, T. R.; Lee, M. S.; Lee, A. M.; Gwaltney, S. R.; Adams, T. R.; Ochsenfeld, C.; Gilbert, A. T. B.; Kedziora, G. S.; Rassolov, V. A.; Maurice, D. R.; Nair, N.; Shao, Y. H.; Besley, N. A.; Maslen, P. E.; Dombroski, J. P.; Daschel, H.; Zhang, W. M.; Korambath, P. P.; Baker, J.; Byrd, E. F. C.; Van Voorhis, T.; Oumi, M.; Hirata, S.; Hsu, C. P.; Ishikawa, N.; Florian, J.; Warshel, A.; Johnson, B. G.; Gill, P. M. W.; Head-Gordon, M.; Pople, J. A. *J. Comput. Chem.* **2000**, *21*, 1532−1548.

(26) Hehre, W. J.; Ditchfield, R.; Radom, L.; Pople, J. A. *J. Am. Chem. Soc.* **1970**, *92*, 4796−4801.

(27) Raghavachari, K.; Trucks, G. W.; Pople, J. A.; Head-Gordon, M. *Chem. Phys. Lett.* **1989**, *157*, 479.

(28) (a) Klopper, W.; Bak, K. L.; Jorgensen, P.; Olsen, J.; Helgaker, T., *J. Phys. B* **1999**, *32*, R103−R130. (b) Paldus, J.; Li, X. Z. *Adv. Chem. Phys.* **1999**, *110*, 1−175.

(29) (a) Feyereisen, M.; Fitzgerald, G.; Komornicki, A. *Chem. Phys. Lett.* **1993**, *208*, 359−363. (b) Weigend, F.; Haser, M.; Patzelt, H.; Ahlrichs, R. *Chem. Phys. Lett.* **1998**, *294*, 143−152.

(30) (a) Runge, E.; Gross, E. K. U. *Phys. Rev. Lett.* **1984**, *52*, 997. (b) Bauernschmitt, R.; Ahlrichs, R. *Chem. Phys. Lett.* **1996**, *256*, 454−464. (c) Hirata, S.; Head-Gordon, M. *Chem. Phys. Lett.* **1999**, *302*, 375−382.

(31) Zaitsev, V. Unpublished results.

(32) Note, however, that absorption spectra of solutions containing radical are contaminated by temperature-independent absorption band of small admixtures of byproducts, which are characterized by extremely high extinction coefficients of $\sim 10^5$ $M^{-1}$ $cm^{-1}$.

(33) Kristyan, S.; Pulay, P. *Chem. Phys. Lett.* **1994**, *229*, 175−180.

(34) Perrin, D. D.; Armagero, W. L.; Perrin, D. R. *Purification of Laboratory Chemicals*, 2nd ed; Pergamon: New York, 1980.